Electronic Supplementary Information (ESI)

Bioinspired Elastic Piezoelectric Composite for High-Performance Mechanical Energy Harvesting

Yong Zhang,‡[a,b] Chang Kyu Jeong,‡[b,c] Tiannan Yang,[b] Huajun Sun,[a] Long-Qing Chen,[b] Shujun Zhang,[b,d] Wen Chen,*[a] Qing Wang*[b]

[a] *Center for Smart Materials and Device Integration, State Key Laboratory of Advanced Technology for Materials Synthesis and Processing, School of Materials Science and Engineering, Wuhan University of Technology, Wuhan 430070, China*

[b] *Department of Materials Science and Engineering, The Pennsylvania State University, University Park, PA 16802, United States*

[c] *Division of Advanced Materials Engineering, Chonbuk National University, Jeonju, Jeonbuk 54896, Republic of Korea*

[d] *Institute for Superconducting and Electronic Materials, Australian Institute of Innovative Materials, University of Wollongong, Wollongong, New South Wales 2500, Australia*

*****E-mail: chenw@whut.edu.cn (W. Chen), wang@matse.psu.edu (Q. Wang)

‡These authors contributed equally to this work.

Experimental Section

Chemicals. Barium acetate ($Ba(CH_3COO)_2$, 99%), calcium acetate monohydrate ($Ca(CH_3COO)_2 \cdot H_2O$, 99%), zirconium (IV) propoxide solution (70 wt % in 1-propanol) and glacial acetic acid (CH_3COOH, 99%) were supplied by Sigma-Aldrich. Titanium (IV) n-butoxide ($C_{16}H_{36}O_4Ti$, 99%) was purchased from Acros Organics. Polydimethylsiloxane (PDMS, Sylgard 184) was bought from Dow Corning. All chemicals were used without purification.

BCZT sol-gel synthesis. Barium acetate and calcium acetate monohydrate were dissolved in glacial acetic acid at 80 ^oC for 3 h. Zirconium (IV) propoxide solution and titanium (IV) n-butoxide were mixed together for half an hour. Then two mixtures were blended for another two hours to form a clear yellowish sol-gel. The concentration was finally adjusted as 0.1 M.

Characterization and measurements. The mechanical stimulations of the PCG as well as the analyses of strain-stress curves and Young's moduli were conducted by a TA Instrument RSA-G2 solids analyzer. The electrical output signals were measured by an electrometer (Keithley 6514) with the cyclic stimulation by the RSA-G2 dynamic motion.

Phase-field modeling based on a Fourier spectral iterative perturbation method

The phase-field simulation based on a Fourier spectral iterative perturbation method is conducted to provide theoretical evidence on the mechanism of the enhanced piezoelectric effect in the PDMS/BCZT foam composites. By applying an external compressive strain ε_{33} = -0.12, the induced stress is concentrated in the BCZT phase in both particle and foam composites. However, due to the interconnected BCZT phase structure, the foam composite shows a much higher deformation and stress in the BCZT phase than the particle composite. For comparison, the average stress in the foam composite is σ_{avg} = -0.80 MPa, 4 times larger than the particle composite at σ_{avg} = -0.18 MPa. This larger induced stress would generate a stronger piezoelectric polarization, and as a result, stronger piezoelectric voltage response. Compared with the particle composite where the electric field (i.e. piezoelectric voltage response) is only concentrated in small regions adjacent to the BCZT particles while remains weak in the PDMS matrix, the foam composite shows a generally stronger electric field throughout both the BCZT and PDMS phases. The total piezoelectric voltage response in the foam composite is E_{avg} = 613 kV/m, with a ~ 4 times enhancement from that of the particle composite at E_{avg} = 165 kV/m, which agrees well with our experimentally observed voltage response enhancement.

In the phase-field model, the total the simulation system is discretized into a three-dimensional array of 120 × 120 × 120 grid points. A three-dimensional periodic boundary condition is applied. Two types of structures are considered with spherical BCZT particles randomly distributed in a PDMS matrix, and interconnected porous BCZT foam structures in a PDMS matrix, respectively. The spatial distribution of electric field $\mathbf{E}(\mathbf{r})$, polarization $\mathbf{P}(\mathbf{r})$, stress $\boldsymbol{\sigma}$ and strain $\boldsymbol{\varepsilon}$ in the composite responsive to an external electric field is modeled through solving the electrostatic equilibrium equation[1]

$$\nabla \cdot \mathbf{D} = \nabla \cdot \left(\varepsilon_0 \boldsymbol{\kappa}_r \mathbf{E} + \mathbf{d}\boldsymbol{\sigma} \right) = \mathbf{0} \tag{1}$$

and the elastic equilibrium equation

$$\nabla \cdot \boldsymbol{\sigma} = \nabla \cdot \left(\mathbf{c}\boldsymbol{\varepsilon} - \mathbf{d}^T \mathbf{E} \right) = \mathbf{0} \tag{2}$$

where ε_0 is the vacuum dielectric permittivity, $\boldsymbol{\kappa}_r(\mathbf{r})$, $\mathbf{d}(\mathbf{r})$, and $\mathbf{c}(\mathbf{r})$ are relative dielectric permittivity, piezoelectric coefficient, and elastic stiffness of the local phase, respectively. Equations (1) and (2) are iteratively solved using the Fourier spectral iterative perturbation method.[2,3] The material constants are chosen as follows. For PDMS, $\kappa_r = 2.5$, $d_{33} = 0$, and $c_{11} = 1.02\text{MPa}$; for BCZT, $\kappa_r = 3000$, $d_{33} = 620\text{pC/N}$, and $c_{11} = 1.72\text{GPa}$.

The effective strain efficiency (ESE) of particle-based composite

Regarding the entire structure is subjected to an external applied stress ε_{33},[4,5] the effective strain on the BCZT particle filler can be described as,

$$\varepsilon_{33}^{BCZT} = \frac{A+B}{A+B/k}\varepsilon_{33} \tag{3}$$

where A and B are geometrical factors of BCZT particle and PDMS part.

Usually, k is much smaller than 1, and A can be simplified in the same order of B (A~B). Therefore, the ESE can be defined as,

$$\eta_{\text{ptc}} = \frac{k}{1-\sqrt[3]{\varphi}} \tag{4}$$

where $\varphi \equiv \left(\frac{A}{A+B}\right)^3$ depicts the volume fraction of BCZT particles in the composite. Based on the typical and experimental values, k = 1/60000 and φ = 0.16 can be set, then the ESE is about 4×10^{-5}.

The Young's modulus and ESE of 3D porous composite

First, the effective Young's modulus of the 3D porous structured composite can be calculated by multiplying the Young's modulus of BCZT and the fraction of stress on the directly forced BCZT based on the Banno unit cell model,[4-6] as follow,

$$E^* = E^{BCZT}\frac{1}{(1+R_a)^2}\left[1+\frac{{R_a}^2}{k}+\frac{2R_a(1+R_a)}{1+kR_a}\right]^{-1} \tag{5}$$

where R_a is the aspect ratio of the frame of 3D structure. Based on the typical and experimental values, $R_a \approx 3$, E^{BCZT} = 60-70 GPa and $k \ll 1$, the effective Young's modulus of 3D porous composite is estimated as 2-3 MPa. In the classical mechanics, the composites are considered as homogeneous orthotropic media with certain effective moduli which indicate the mean mechanical

properties of the composites.

When the 3D composite is under the uniaxial stress, the ESE can be estimated by,

$$\eta_{3D} \cong \sqrt{\frac{E^*}{\varphi E^{BCZT}}} \tag{6}$$

Based on the Banno cell model, the volume fraction can be expressed by the aspect ratio,

$$\varphi = \frac{1+3R_a}{(1+R_a)^3} \tag{7}$$

Hence, the ESE is finally described as follow.

$$\eta_{3D} \cong \sqrt{\frac{1+R_a}{1+3R_a}\left(1 + k{R_a}^2 + \frac{2R_a(1+R_a)}{1+R_a/k}\right)} \tag{8}$$

Because $\varphi = 0.16$, $R_a \approx 3$, and $k \ll 1$ experimentally, the ESE is calculated as ~0.63. However, it should be calibrated because some of PDMS buffer layers are inevitably involved onto the composite. Considering the ratio of thickness of PDMS buffer layer (t) is 5%, the actual ESE can be finally defined as below.[5]

$$\eta^*_{3D} \approx \eta_{3D}\frac{(1+R_a)^2 k}{t} \approx 3 \times 10^{-3} \tag{9}$$

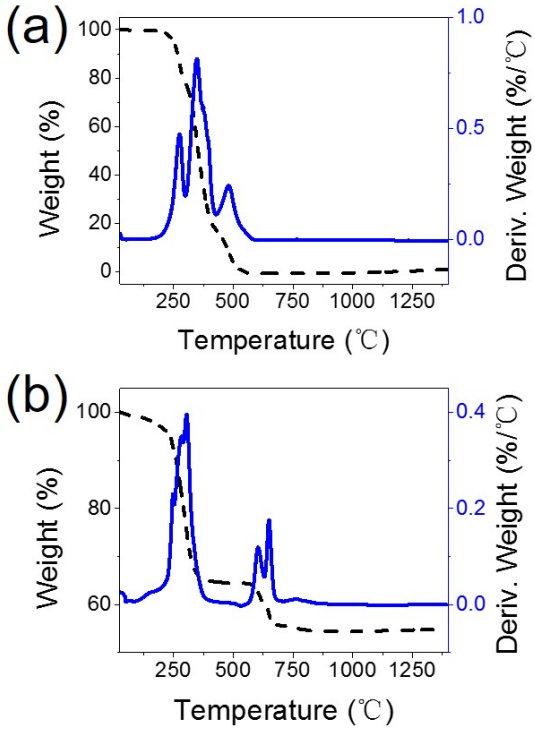

Fig S1. Thermogravimetric analysis of (a) sponge template and (b) BCZT sol-gel.

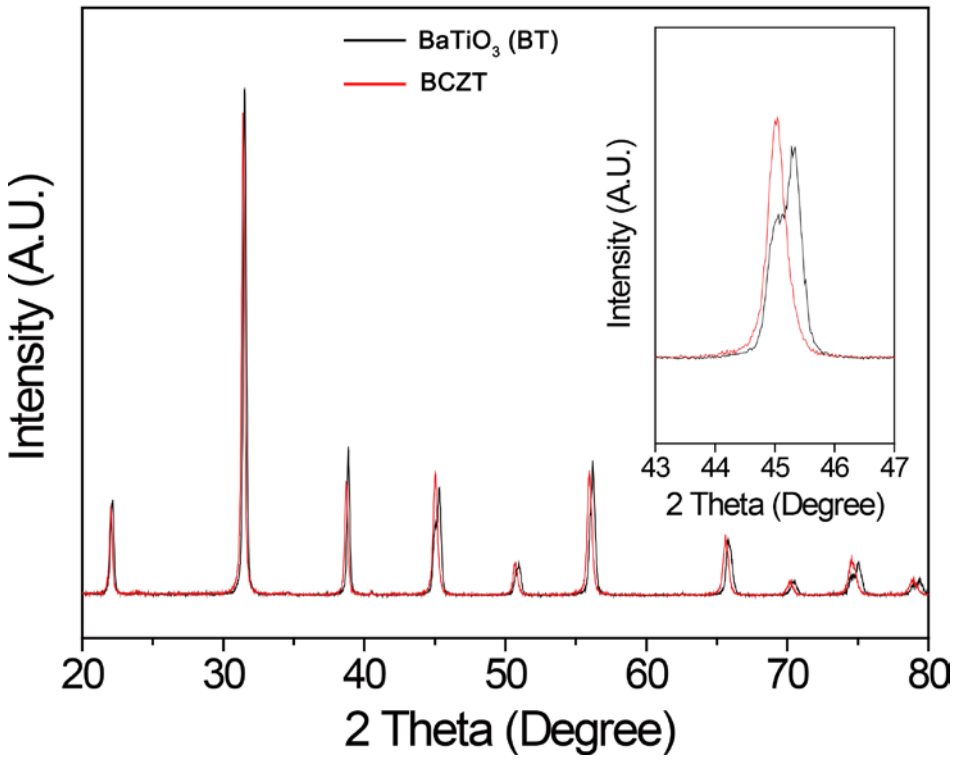

Fig S2. High resolution XRD patterns of BT and BCZT. Inset: the magnified XRD scan showing (200) peaks of each material. Because BT has only tetragonal phase, there is peak splitting (existence of peak shoulders). In contrast, there is no peak splitting in the case of BCZT because the MPB from a rhombohedral-tetragonal fused region cannot show definite peak shoulders.[7-9] Additionally, the XRD pattern of BCZT presents peak shifting to lower angles, compared to that of BT. This is due to the change of interplanar spacing caused by the size effects of Zr^{4+} and Ca^{2+} ions.[9,10]

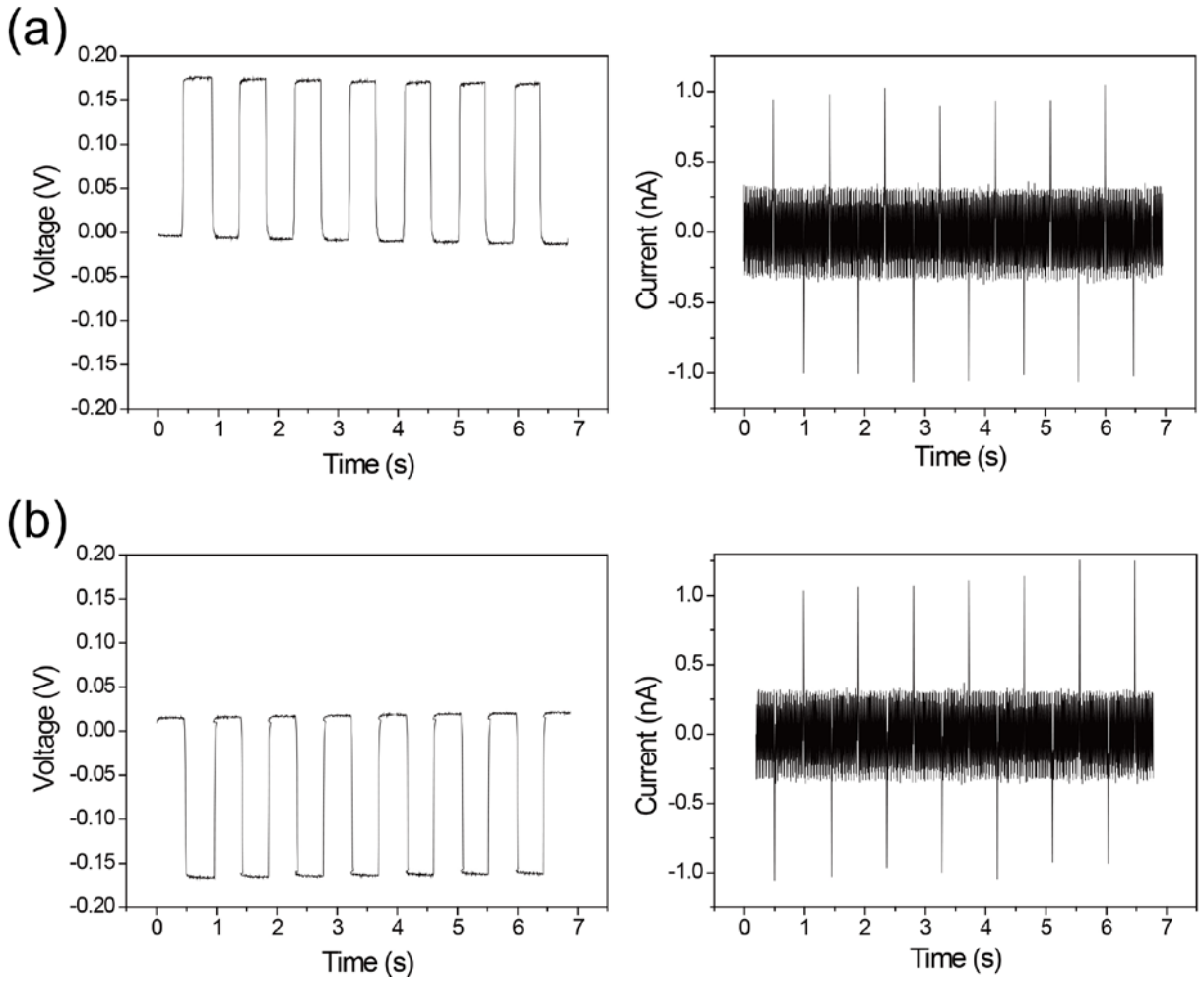

Fig S3. Energy harvesting peaks generated from the PU sponge-PDMS composite device to investigate the triboelectric influence. Voltage and current peaks with (a) forward connection and (b) reverse connection.

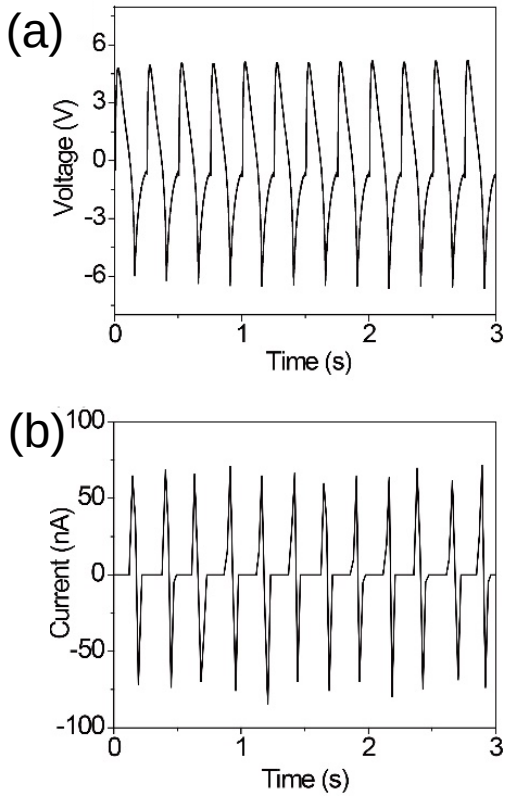

Fig S4. (a) The open-circuit output voltage and (b) the short-circuit current of the randomly-dispersed particle composite generator.

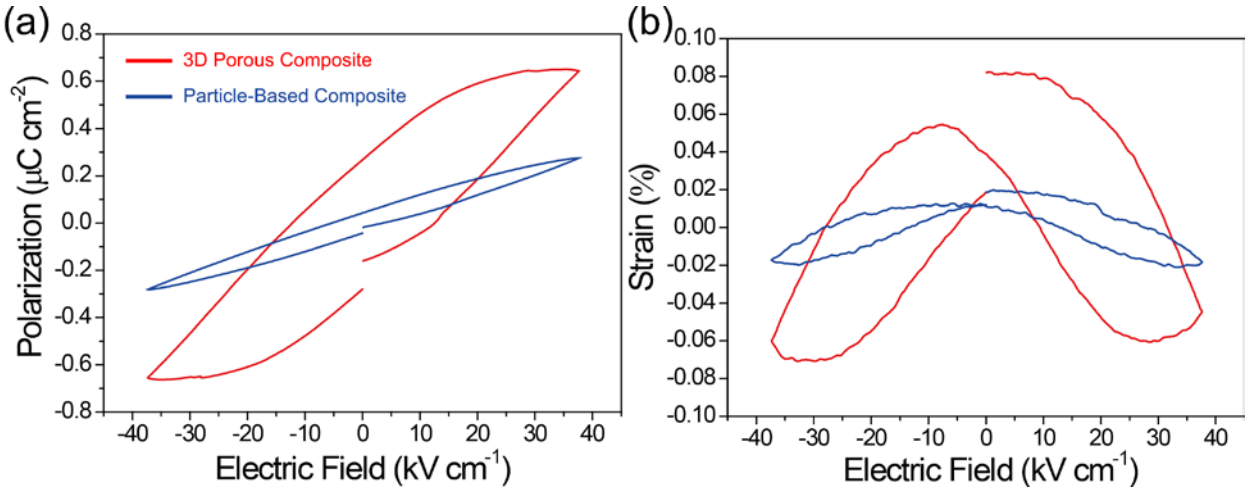

Fig S5. (a) Polarization hysteresis and (b) strain loop curves of the 3D porous composite and the randomly dispersed particle-based composite.

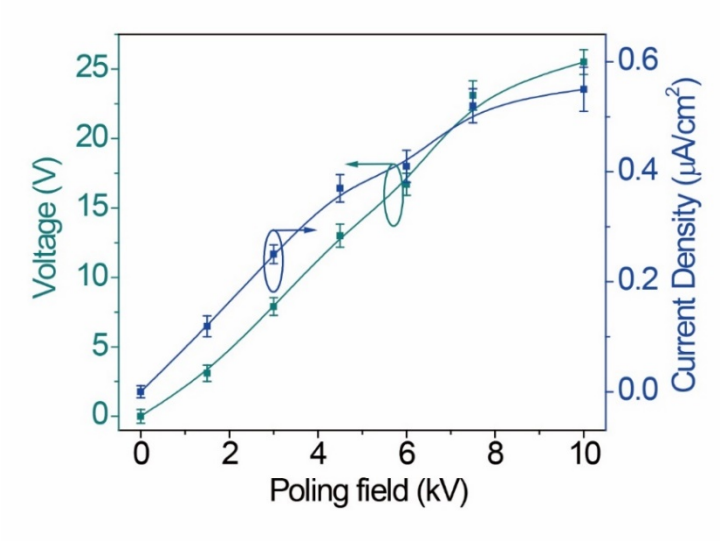

Fig S6. Output voltage and current density as a function of poling field. 10 kV is the limitation of the poling instrument.

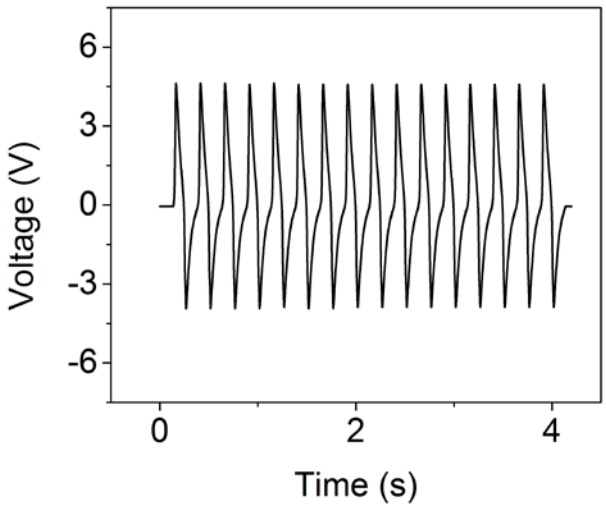

Fig S7. The output voltage generated under 7% tensile strain.

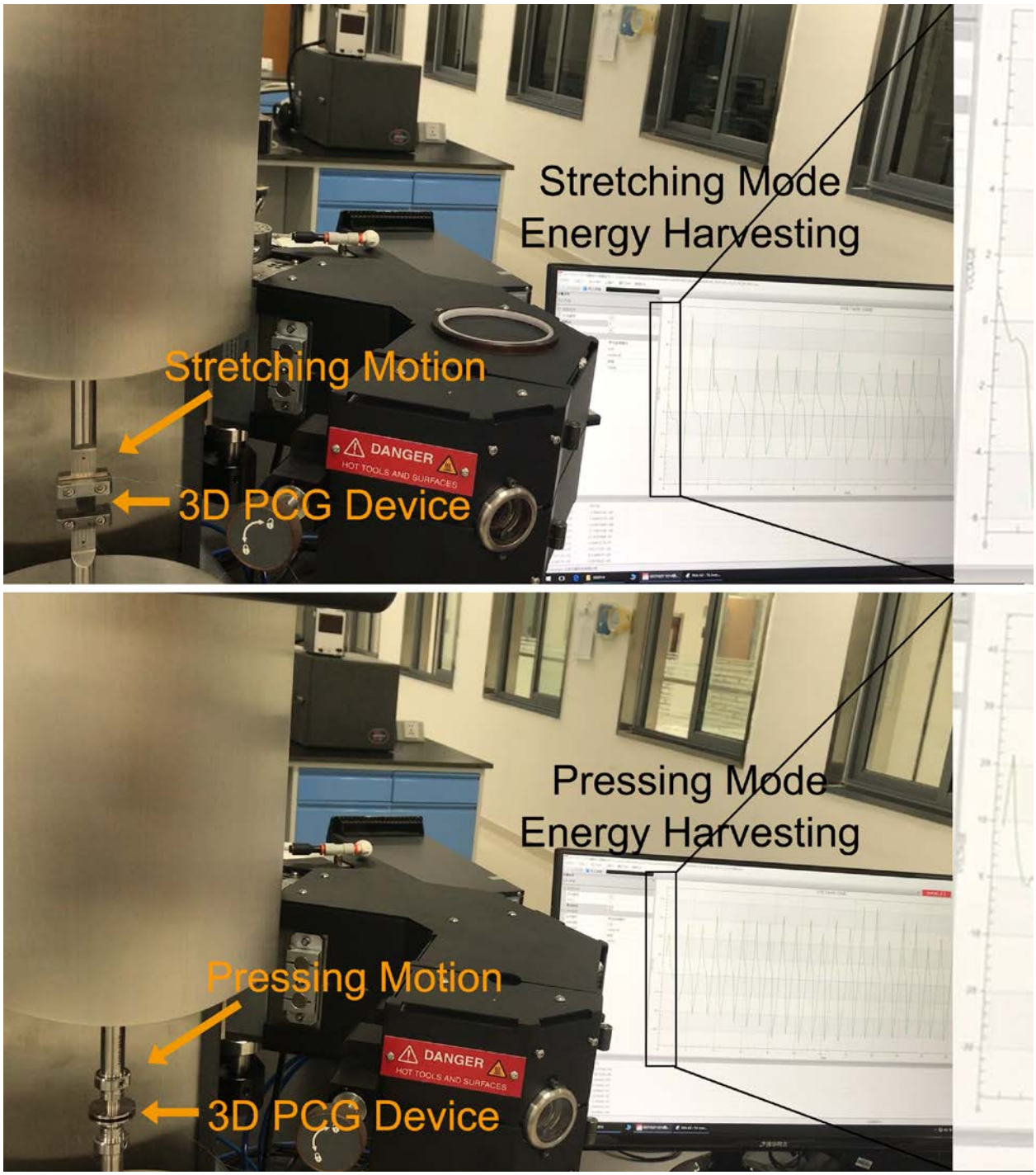

Fig S8 (Video S1). High-definition and enlarged captured pictures from the original file of supporting video. A supplementary video is uploaded, which shows the energy harvesting from the 3D PCG device in stretching and pressing mechanical stimulations, respectively. Due to the restriction of uploaded file size (only available for a mid-definition video), these high-definition captures are also attached as above. Detailed behavior is shown in the supplementary video file.

Supporting References

1. Y. L. Li, S. Y. Hu, Z. K. Liu and L. Q. Chen, *Appl. Phys. Lett*., 2002, **81**, 427.

2. J. J. Wang, X. Q. Ma, Q. Li, J. Britson and L. Q. Chen, *Acta Mater.*, 2013, **61**, 7591.

3. S. Y. Hu and L. Q. Chen, *Acta Mater.*, 2001, **49**, 1879.

4. C. R. Bowen, A. Perry, H. Kara and S. W. Mahon, *J. Eur. Ceram. Soc.*, 2001, **21**, 1463.

5. G. Zhang, P. Zhao, X. Zhang, K. Han, T. Zhao, Y. Zhang, C. K. Jeong, S. Jiang, S. Zhang and Q. Wang, *Energy Environ. Sci.*, 2018.

6. K. Rittenmyer, T. Shrout, W. A. Schulze and R. E. Newnham, *Ferroelectrics*, 1982, **41**, 189.

7. D. Damjanovic, A. Biancoli, L. Batooli, A. Vahabzadeh and J. Trodahl, *Appl, Phys, Lett.*, 2012, **100**, 192907.

8. A. P. Turygin, M. M. Neradovskiy, N. A. Naumova, D. V. Zayats, I. Coondoo, A. L. Kholkin and V. Y. Shur, *J. Appl. Phys.*, 2015, **118**, 072002.

9. L. Liu, S. Zheng, Y. Huang, D. Shi, S. Wu, L. Fang, C. Hu and B. Elouadi, *J. Phys. D*, 2012, **45**, 295403.

10. C. Baek, J. E. Wang, S. Ryu, J.-H. Kim, C. K. Jeong, K.-I. Park and D. K. Kim, *RSC Adv.*, 2017, **7**, 2851.